IJP

Nuclear structure effects in parity non-conservation in heavy ions

P K Panda[1]* and B P Das[2]

[1]Raman Center for Atomic, Molecular and Optical Sciences, Indian Association for the Cultivation of Science,
Jadavpur, Kolkata-700 032, India
[2]Indian Institute of Astrophysics, II Block, Koramangala, Bangalore-560 034, India

e-mail : prafulla.k.panda@gmail.com

Abstract : We calculate the binding energy, charge radii in $^{129}Ba-^{143}Ba$ and $^{214}Ra-^{226}Ra$ using the relativistic mean field theory which includes scalar and vector mesons We then evaluate the nuclear structure corrections to the weak charges for a series of these isotopes using different parameters and estimate their uncertainty in the framework of this model Our results will have important implication for the ongoing and planned parity non-conservation experiments and atomic structure calculations on Ba^+ and Ra^+

1. Introduction

Parity non-conservation (PNC) in heavy atoms have provided an important confirmation [1–3] of the SU(2) × U(1) electro-weak sector of the Standard Model (SM). By combining the results of precision measurements and calculations using sophisticated many-body methods [4–6], it is possible to extract the nuclear weak charge and compare with its corresponding value in the SM. A discrepancy between these two values could reveal the possible existence of new physics beyond the SM [7].

As first pointed out by Bouchiat and Bouchiat [1], the matrix element of the PNC Hamiltonian scales as Z^3. It is primarily because of this reason that heavy atoms are considered to be the best candidates for PNC experiments. A high precision measurement of PNC in atomic cesium [3] has reduced significantly the uncertainty (< 1%) in the determination of the nuclear weak charge, Q^W, of the Cs nucleus and

the deviation from the SM is about 1σ [8]. It would also be desirable to consider other systems that have the potential to yield accurate values of the nuclear weak charge. Ba^+ and Ra^+ deserve special mention in this context The transition of interest are $6s^2S_{1/2} \rightarrow 5d^2D_{3/2}$ for Ba^+ and $7s^2S_{1/2} \rightarrow 6d^2D_{3/2}$ for Ra^+. An experiment is underway for Ba^+ using the techniques of ion trapping and laser cooling and another has been proposed for Ra^+ [9,10] Relativistic many-body calculations [11–13] have also been carried out on these two ions

The experimental result needs input from atomic structure calculations involving the interplay of electromagnetic and weak interactions. However, the small but non-negligible effects of nuclear size must be addressed before an interpretation of PNC data in terms of the fundamental electro-weak couplings is possible. Thus nuclear structure could become a crucial factor in the interpretation of PNC experiments with increasing accuracy [14–18]. An extensive discussion on the sensitivity of atomic PNC and electric dipole moments to possible new physics has been recently reported in Ref. [19]

There have been earlier studies to determine nuclear structure effects in PNC in atomic cesium using non-relativistic potentials [16,17] as well as relativistic models [18]. In this paper we present a relativistic calculation of these effects for the Ba and Ra isotopes using the relativistic mean field theory (RMF). It is motivated by the current efforts to observe PNC in Ba^+ and Ra^+ and also to yield interesting information on neutron distributions

The RMF theory, which was first proposed by Teller and co-workers [20–22] and later by Walecka [23] and developed by others, has been fairly successfully applied to both nuclear matter and finite nuclei The method gives good description for binding energies, root mean square (rms) radii, quadruple and hexadecapole deformations and other nuclear properties not only for the spherical, but also for the deformed nuclei The same parameter set of the model also describes well the properties of nuclear matter. One of the major attractive features of the RMF approach is the incorporation of the spin-orbit interaction due to to the presence of the one body Dirac Hamiltonian and the nuclear shell structure automatically arises from the nucleon-nucleon interaction *via* the scalar and vector mesons We can therefore expect the RMF calculation to provide useful information on nuclear structure corrections to atomic PNC.

We organize the paper as follows · in Section 2, we describe the PNC in standard model, Section 3 contains briefly the RMF model for nuclear theory, results and discussion are described in Section 4

2. PNC in standard model

In the Standard Model, the electron-nucleon interaction is mediated by both the photon and the intermediate boson Z^0. The latter does not conserve parity. The energy

Involved in the atomic PNC experiments are usually only a fraction of an eV, while the mass of the Z^0 is $\simeq$ 92 GeV, and thus the parity non-conserving interaction may be written as a contact interaction. We have the effective Hamiltonian

$$H_{pnc} = \frac{G_F}{\sqrt{2}} \sum_{eB} \left[C_{1B} \int \psi_B^\dagger \psi_B \psi_e^\dagger \gamma_5 \psi_e d^3r + C_{2B} \int \psi_B^\dagger \sigma_B \psi_B \cdot \psi_e^\dagger a \psi_e d^3r \right], \tag{1}$$

where B stands for n (neutron) or p (proton). The first term grows coherently with nucleon numbers N and Z. The second term together with the anapole moment term amounts to at most a few percent of the first term in heavy atoms. We shall therefore consider only the first term. The effective Hamiltonian becomes

$$H_{pnc} = \frac{G_F}{\sqrt{2}} \int \left[NC_{1n}\rho_n(r) + ZC_{1n}\rho_p(r) \right] \psi_e^\dagger \gamma_5 \psi_e d^3r, \tag{2}$$

where the proton and neutron densities, $\rho_{p,n}(r)$, are normalized to unity. We have assumed the Standard Model nucleon couplings $C_{1p} \equiv 2C_{1u} + C_{1d} = \frac{1}{2}(1 - 4\sin^2\theta_W)$;

$C_{1n} \equiv 2C_{1u} + C_{1d} = -\frac{1}{2}$, where $\sin^2\theta_W$ is the Weinberg mixing angle. We need the spatial variation of the electron part $\psi_e^\dagger \gamma_5 \psi_e$ over the nucleus, its normalization and its dependence on nuclear structure. PNC effects are dominated by s-electrons ($\kappa = -1$) coupled to p-electrons ($\kappa = 1$). This can be expressed as $\rho_5(r) \equiv \psi_p^\dagger \gamma_5 \psi_s = \mathcal{A}(Z)\mathcal{N}(Z,R)f(r)$, where $\mathcal{A}(Z)$ contains all atomic-structure effects for a point nucleus including many-body correlations, $\mathcal{N} \equiv \psi_p^\dagger(0)\gamma_5\psi_s(0)$ is the normalization factor for single electron and $f(r)$ describes the spatial variation. It is the integrals

$$q_{n,p} = \int f(r)\rho_{n,p}(r)d^3r, \tag{3}$$

which determine the effect of the proton and neutron distributions on the PNC observables. From eq. (2), the matrix element between two atomic states i and j are given by,

$$\langle i | H_{pnc} | j \rangle = \frac{G_F}{2\sqrt{2}} \mathcal{A}(Z)\mathcal{N} \left[Q_W(N,Z) + Q_W^{nuc}(N,Z) \right], \tag{4}$$

where $Q_W(N,Z)$ is the weak charge. For the Standard Model, the weak charge takes the form at tree level as

$$Q_W(N,Z) = -N + Z(1 - 4\sin^2\theta_W). \tag{5}$$

The nuclear structure correction $Q_W^{nuc}(N,Z)$ describes the part of the PNC effect that arises from the finite nuclear size. In the same approximation as (5) above

$$Q_W^{nuc}(N, Z) = -N(q_n - 1) + Z(1 - 4\sin^2\theta_W)(Q_p - 1). \tag{6}$$

The proton (charge) nuclear form factors needed for q_p and $\mathcal{N}$ are generally well known from the measurements of the charge distribution of nuclei close to the stable valley and many unstable nuclei as well. The neutron nuclear form factor needed for q_n is not well determined experimentally and is model dependent. To estimate the importance of PNC in nuclear structure, the form factor can be approximated to the order of $(Z\alpha)^2$ for a sharp nuclear surface, and neglecting the electron mass in

comparison with the nuclear Coulomb potential [15], $f(r) \simeq 1 - \dfrac{1}{2}(Z\alpha)^2 \times$

$\left[(r/R^2) - \dfrac{1}{5}(r/R)^4 + \dfrac{1}{75}(r/R)^6 \right]$. For a sharp nuclear surface density distribution, the

only relevant parameter is the nuclear radius R and $\langle r^{2n} \rangle = 3/(2n + 3n)R^{2n}$

One of the motivations for further improving atomic PNC experiments is to test the Standard Model parameters After the inclusion of radiative corrections, we begin by rewriting eqs (8) and (9) in the form

$$Q_W(N, Z) = 0.9878 \times \left[-N + Z(1 - 4.0118\bar{x}) \right] \times (1.0 + 0.00782T), \tag{7}$$

$$\bar{x} = 0.23124 \pm 0\,00017 \pm 0.003636S - 0.00258T, \tag{8}$$

where $\bar{x}$ is assumed here to be defined at the mass scale M_Z by modified minimal subtraction [7], S is the parameter characterizing the isospin conserving new quantum loop corrections and T characterizing isospin breaking corrections. The nuclear structure correction to Q_W is given by

$$Q_W^{nuc}(N, Z) = 0.9878 \times \left[-N(q_n - 1) + Z(1 - 4.0118\bar{x})(q_p - 1) \right]. \tag{9}$$

The coefficients $q_{n,p}$ defined earlier in eq. (6) contain the nuclear structure effects. We have also included the intrinsic nucleon structure contributions in evaluating the nuclear structure correction as in Ref. [16].

3. Relativistic mean field theory

The relativistic Lagrangian density for a nucleon-meson many-body system [24–26] is

$$\mathcal{L} = \bar{\psi}_i \left(i\gamma^\mu \partial_\mu - M \right) \psi_i$$

$$+ \frac{1}{2} \partial^\mu \sigma \partial_\mu \sigma - \frac{1}{2} m_\sigma^2 \sigma^2 + \frac{1}{3} g_2 \sigma^3 + \frac{1}{4} g_3 \sigma^4 - g_s \bar{\psi}_i \psi_i \sigma$$

$$- \frac{1}{4} \Omega^{\mu\nu}\Omega_{\mu\nu} + \frac{1}{2} m_\omega^2 \omega^\mu \omega_\mu \frac{1}{4} c_3(\omega_\mu\omega^\mu)^2 - g_\omega \bar{\psi}_i \gamma^\mu \psi_i \omega_\mu$$

$$-\frac{1}{4}B^{\mu\nu}\ B_{\mu\nu}+\frac{1}{2}m_\rho^2 R^\mu\ R_\mu-g_\rho\bar{\psi}_i\gamma^\mu\tau\psi_i\cdot R^\mu$$

$$-\frac{1}{4}F^{\mu\nu}F_{\mu\nu}-e\bar{\psi}_i\gamma^\mu\ \frac{(1-\tau_{3i})}{2}\ \psi_i A_\mu. \tag{10}$$

The field for the σ-meson is denoted by σ, that of the ω-meson by ω_μ and of the iso-vector ρ-meson by R_μ. A^μ denotes the electromagnetic field. ψ_i are the Dirac spinors for the nucleons, whose third component of isospin is denoted by τ_{3i}. Here g_s, g_ω, g_ρ and $e^2/4\pi = 1/137$ are the coupling constants for σ, ω, ρ mesons and photon respectively. M is the mass of the nucleon and m_σ, m_ω and m_ρ are the masses of the σ, ω and ρ mesons respectively. $\Omega^{\mu\nu}$, $B^{\mu\nu}$ and $P^{\mu\nu}$ are the field tensors for the ω^μ, ρ^μ and the photon fields respectively. The field equations for mesons and nucleons are obtained from the Lagrangian of eq. (10) and can be found in Ref [25]. These are nonlinear, coupled partial differential equations, which are solved self-consistently. These equations are solved by expanding the upper and lower components of the Dirac spinors ψ_i and the boson fields wave functions in terms of a deformed harmonic oscillator potential basis.

The total binding energy of the system is

$$E_{tot}=E_{part}+E_\sigma+E_\omega+E_\rho+E_C+E_{pair}+E_{cm} \tag{11}$$

where E_{part} is the sum of single particle energies of the nucleons, E_σ, E_ω, E_ρ are the contributions of meson energies, and E_C and E_{pair} are the coulomb and pairing energy respectively. We have used the pairing gap defined in Ref. [27] to take pairing in to account. $E_{cm}-\ -\frac{3}{4}41A^{-1/3}$ is the non-relativistic approximation for the center-of-mass correction.

4. Results and discussion

In this section, we apply RMF theory with TM1, NL3 and NL-SH interactions to study the ground state properties of Ba and Ra isotopes These elements have an important implications for the PNC experiments and atomic structure calculations. The parameters of these interactions are given in Table 1. We note that in TM1 parameter set has the non-negative value of the quartic self-coupling coefficient g_3 for the omega mesons In most of the successful parameter sets the quartic self-coupling term for sigma meson is negative, so that the energy spectrum is unbounded below. Although in normal cases the solutions are obtained in local minimum, all these parameter sets give a good account on various properties such as binding energy, compressibility, asymmetric energy for nuclear matter.

In Tables 2, 3 and 4, binding energies, charge radius and shift $\delta r_{\rho,n}^2$ and $\delta r_{\rho,n}^4$, are listed for the barium isotopes with different interactions. The calculated shift in

Table 1. Parameters used in our calculation.

	TM1	NL3	NL-SH
M	938 0	939 0	939 0
m_σ	511 198	508 194	526 059
m_ω	783 0	782 501	783.0
m_ρ	770 0	763 0	763.0
g_σ	10 0289	10 217	10 444
g_2	--7 2325	--10 431	--6 9099
g_3	0 6183	--28 885	--15 8337
g_ω	12.6139	12 868	12 945
c_3	71 3075	0.000	0 000
g_ρ	4 6322	4 474	4 383

Table 2. Results of RMF calculations for Ba isotopes in TM1 parameter The binding energies are in MeV, all radii are in fm.

N	E_{RMF}	E^a	r_{ch}	r_{ch}^b	$r_n - r_p$	δr_p^2	δr_n^2	δr_p^4	δr_n^4
73	1086 5	1082.4	4 829	4 825	0 137	--0.248	--1 080	11 330	53 032
75	1103 9	1100 2	4 834	4 828	0 157	--0 200	--0 834	9 165	41 177
77	1120 7	1117 2	4.843	4 829	0 178	--0 124	--0.548	5 688	27 197
79	1138 8	1133 6	4 849	4 827	0.201	--0.057	--0.249	2 631	12 473
81	1155 3	1149 7	4 855	4 832	0 220	0.00	0 00	0 00	0 00
83	1167 6	1163 0	4 872	4 852	0.238	0 163	0 352	7 058	17 780
85	1177 2	1173 9	4 902	4 882	0 256	0 452	0 838	20.954	42.773
87	1187 3	1184 3	4 929	4 911	0.271	0 723	1 276	33.732	65 771

*Ref [28], *Ref [29].

Table 3. Same as Table 2 for Ba isotopes in NL3 parameter

N	E_{RMF}	E^a	r_{ch}	r_{ch}^b	$r_n - r_p$	δr_p^2	δr_n^2	δr_p^4	δr_n^4
73	1082.2	1082 4	4.820	4 825	0.140	--0 171	--1.048	7 775	51 307
75	1098 9	1100 2	4 819	4 828	0 162	--0 171	--0 833	7 775	40 928
77	1118 9	1117 2	4 826	4 829	0 183	--0 105	--0 557	4 762	27 516
79	1136.4	1133 6	4 833	4 827	0 208	--0 047	--0 249	2 168	12 399
81	1152.4	1149.7	4 837	4.832	0.228	0 00	0 00	0 00	0.0000
83	1165 1	1163 0	4 854	4 852	0 248	0 162	0 371	7 424	18 695
85	1173 6	1173 9	4 886	4 882	0 269	0 470	0.908	21 616	46 202
87	1184.1	1184 3	4 910	4 911	0 296	0 712	1 440	32 901	74.038

neutron radii are also listed in Tables 2 (TM1), 3 (NL3) and 4 (NL-SH) for barium isotopes. In Tables 5, 6 and 7, binding energies, charge radius and shift $\delta r_{p,n}^2$ and $\delta r_{p,n}^4$ are listed for the radium isotopes with different parameter sets. We have also

Table 4 Same as Table 2 for Ba isotopes in NL-SH parameter

N	E_{RMF}	E^a	r_{ch}	r^b_{ch}	$r_n - r_p$	δr^2_p	δr^2_n	δr^4_p	δr^4_n
73	1085 8	1082 4	4 801	4 825	0 133	−0 218	−1 003	9 832	48 537
75	1106 1	1100 2	4 805	4 828	0 153	−0 180	−0 769	8 132	37.387
77	1123 2	1117 2	4 812	4 829	0 173	−0 114	−0 504	5 147	24 646
79	1139.7	1133 6	4 818	4 827	0 194	−0 057	−0 237	2 578	11 693
81	1157 7	1149 7	4 823	4 832	0 212	0 000	0 000	0 000	0 000
83	1170 5	1163 0	4 841	4 852	0 234	0.162	0 389	7 359	19 366
85	1178 5	1173 9	4 870	4 882	0 251	0 449	0 862	20 539	43 314
87	1188.2	1184 3	4 897	4 911	0 258	0 709	1 207	32 614	61.059

Table 5. Results of RMF calculations for Ra isotopes in TM1 parameter The binding energies are in MeV, all radii are in fm

N	E_{RMF}	E^a	r_{ch}	r^b_{ch}	$r_n - r_p$	δr^2_p	δr^2_n	δr^4_p	δr^4_n
126	1670 1	1658 3	5.642	5.570	0 197	−1 229	−1 982	78 207	136 513
128	1681 8	1671 2	5 658		0 211	−1 050	−1 635	67 010	113 136
130	1693 2	1684 0	5 677		0 221	−0 837	−1 297	53 588	90 191
132	1707 2	1696 5	5 698	5 631	0.229	−0 589	−0 946	37 876	66 093
134	1719.3	1708 7	5 717	5 650	0 239	−0 375	−0.604	24 157	42.444
136	1728 8	1720 3	5 734	5 667	0 246	−0 182	−0 321	11 765	22.607
138	1738 8	1731 6	5 752	5 684	0 257	0 00	0 00	0 00	0 0000
140	1747 9	1742 5	5 766	5 700	0 270	0 182	0.346	11.865	24.626

Table 6. Same as Table 5 for Ra isotopes in NL3 parameter

N	E_{RMF}	E^a	r_{ch}	r^b_{ch}	$r_n - r_p$	δr^2_p	δr^2_n	δr^4_p	δr^4_n
126	1665.9	1658 3	5 621	5 570	0 207	−1 372	−2.134	86 864	146 681
128	1677 6	1671 2	5 638		0 221	−1 183	−1 775	75 097	122 655
130	1687 2	1684 0	5 660		0 231	−0 937	−1 403	59 708	97 448
132	1698 1	1696 5	5 680	5 631	0 241	−0 667	−1 005	42 714	70 206
134	1711 6	1708 7	5 704	5.650	0 252	−0 441	−0 640	28 384	44 952
136	1720 5	1720 3	5 722	5 667	0 264	−0 227	−0 273	14 629	19 297
138	1729 9	1731 6	5 742	5 684	0 267	0 00	0 00	0 00	0 0000
140	1738 1	1742 5	5 757	5 700	0 280	0 170	0.334	11 073	23.795

listed the available experimental binding energies [28] and charge radii [29]. The binding energies agree in all the cases with the experimental values with maximum deviation of 5 to 6 MeV out of a total binding energy of 1000 MeV for barium isotopes and similarly for radium isotopes the deviation for binding energies are around 8 MeV [28] The overall agreement between the theoretical predictions and the experimental values for the charge radii is very good.

Table 7. Same as Table 5 for Ra isotopes in NL–SH parameter.

N	E_{RMF}	E^*	r_{ch}	r^b_{ch}	$r_n - r_p$	δr^2_p	δr^2_n	δr^4_p	δr^4_n
126	1671 7	1658 3	5 603	5 570	0 194	−1 210	−1 910	75 973	129 481
128	1684 2	1671 2	5 618		0 208	−1.042	−1 576	65 596	107.376
130	1694 9	1684 0	5 637		0 218	−0 831	−1 240	52 459	84 936
132	1706 6	1696 5	5 659	5 631	0 226	−0 585	−0 892	37 079	61 364
134	1718 2	1708 7	5 678	5 650	0 235	−0.372	−0 564	23 650	39 034
136	1728 8	1720 3	5 694	5 667	0.244	−0.180	−0 259	11 519	18.009
138	1736 9	1731 6	5 710	5 684	0 250	0 00	0 00	0 00	0 0000
140	1744 6	1742 5	5 725	5 700	0 263	0.158	0 319	10 159	22 379

The difference between proton and neutron radii, neutron thickness, $t = (r_n - r_p)$, are also shown in the Tables. The differences increase with neutron number The lack of unambiguous precise experimental information on the neutron distribution means that one must extrapolate to the desired neutron properties. We note that there is essentially no model independent experimental information on neutron density distributions We next use these radii to estimate the nuclear structure effects in PNC.

The nuclear structure corrections and the weak charge for different isotopes of barium evaluated for $S = T = 0$, are listed in Tables 8 (TM1), 9 (NL3) and 10 (NL-SH)

Table 8. The weak charges $Q_W(N, Z)$, nuclear structure corrections $Q^{nuc}_W(N,Z)$, q_n, q_p and R_n/R_p for Ba isotopes in TM1 parameter

N	$Q_W(N,Z)$	$Q^{nuc}_W(N,Z)$	q_n	q_p	Rn/Rp
73	−68.1093	3 144	0 9546	0 957	1 029
75	−70 0848	3.258	0 9542	0 957	1.033
77	−72 0605	3 376	0 9539	0 957	1 037
79	−74.0361	3 496	0 9536	0 957	1 042
81	−76.0117	3 614	0 9533	0 957	1.046
83	−77.9873	3 731	0.9529	0.957	1 049
85	−79 9629	3 847	0.9527	0.957	1 053
87	−81 9386	3 961	0 9524	0 957	1 056

Table 9. Same as Table 8 for Ba isotopes in NL3 parameter

N	$Q_W(N,Z)$	$Q^{nuc}_W(N,Z)$	q_n	q_p	Rn/Rp
73	−68 1093	3 148	0 9545	0 957	1 029
75	−70.0848	3 265	0 9541	0 957	1 034
77	−72 0605	3.383	0 9538	0.957	1 038
79	−74 0361	3 506	0 9534	0 957	1 044
81	−76.0117	3 626	0.9531	0 957	1 048
83	−77 9873	3 745	0 9528	0.957	1.052
85	−79 9629	3 866	0 9525	0.957	1 056
87	−81.9386	3 997	0 9520	0 957	1 061

Table 10. Same as Table 8 for Ba isotopes in NL–SH parameter

N	$Q_W(N,Z)$	$Q_W^{nuc}(N,Z)$	q_n	q_p	R_n/R_p
73	−68.1093	3 140	0 9546	0 957	1 028
75	−70 0848	3 255	0 9543	0 957	1.032
77	−72 0605	3 371	0 9540	0 957	1.036
79	−74 0361	3 489	0 9536	0 957	1 041
81	−76.0117	3.605	0 9533	0 957	1 044
83	−77.9873	3 727	0 9530	0 957	1.049
85	−79.9629	3 842	0 9527	0 957	1 052
87	−81 9386	3 944	0 9526	0 957	1 053

Table 11. The weak charges $Q_W(N, Z)$, nuclear structure corrections $Q_W^{nuc}(N,Z)$, q_n, q_p and R_n/R_p for Ra isotopes in TM1 parameter

N	$Q_W(N,Z)$	$Q_W^{nuc}(N,Z)$	q_n	q_p	R_n/R_p
126	−118 1770	13.621	0 8865	0 893	1.035
128	−120 1526	13 905	0 8861	0 983	1 037
130	−122 1282	14 174	0 8858	0 893	1 039
132	−124 1038	14 434	0 8855	0 893	1 040
134	−126 0790	14 705	0 8852	0 893	1 042
136	−128 0550	14 962	0 8850	0 893	1 043
138	−130 0306	15 240	0.8847	0 893	1 045
140	−132 0062	15 526	0 8843	0 893	1 047

Table 12. Same as Table 11 for Ra isotopes in NL3 parameter

N	$Q_W(N,Z)$	$Q_W^{nuc}(N,Z)$	q_n	q_p	R_n/R_p
126	−118 1770	13 667	0 8862	0 893	1 037
128	−120 1526	13 952	0 8857	0 983	1.039
130	−122 1282	14 221	0 8854	0 893	1 041
132	−124 1038	14 490	0 8852	0 893	1 042
134	−126 0790	14 766	0 8848	0 893	1 044
136	−128 0550	15 047	0 8844	0 893	1 046
138	−130 0306	15 288	0 8844	0 893	1 047
140	−132 0062	15 577	0 8839	0 893	1 049

for different parameter sets Here one can see that the q_p are constant when the neutron number increases from $N = 73$ to 87. However q_n varies slowly as one increases the neutron number Our RMF calculation gives the nuclear structure correction for ^{137}Ba, Q_W^{nuc} = 3.614 for TM1, 3.626 for NL3 and 3.605 for NL-SH forces. Similarly the nuclear structure correction for ^{226}Ra are Q_W^{nuc} = 15.240 for TM1, 15 288 for NL3 and 15.215 for NL-SH interactions. In Figure 1, we have plotted the nuclear structure corrections *vs* different isotopes of barium (left panel), radium (right

Table 13. Same as Table 11 for Ra isotopes in NL-SH parameter.

N	$Q_W(N,Z)$	$Q_W^{nuc}(N,Z)$	q_n	q_p	R_n/R_p
126	−118 1770	13 614	0 8866	0 893	1 035
128	−120 1526	13 899	0 8861	0 893	1 037
130	−122 1282	14 168	0 8858	0 893	1 039
132	−124 1038	14.428	0 8856	0 893	1 040
134	−126 0790	14 694	0 8854	0.893	1 041
136	−128 0550	14 961	0 8850	0 893	1 043
138	−130 0306	15 215	0 8849	0 893	1 044
140	−132 0062	15 504	0 8845	0 893	1 046
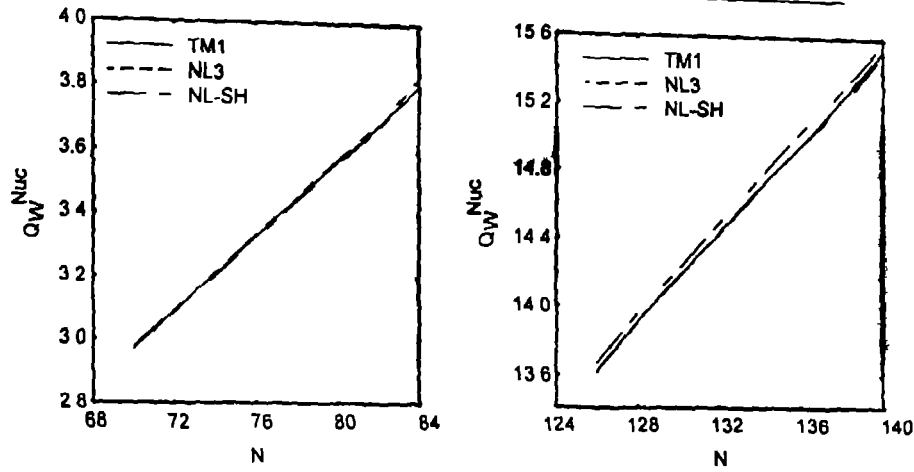
Figure 1. Q_W^{nuc} vs. N for barium isotopes (left panel) and radium isotopes (right panel) in different parameter sets.

panel) for the parameter sets used in our calculations. It is seen that the NL3 parameter gives a higher Q_W^{nuc} compared to other parameters for radium isotopes.

We next discuss explicitly the correction to the weak charge arising from the difference between the neutron and proton distributions. The small difference between q_n and q_p has the effect of modifying the effective weak charge as [30]

$$Q_W = Q_W^{St\ Mod} + \Delta Q_W^{n\ p}$$ (12)

where

$$\Delta Q_W^{n-p} = N(1 - q_n/q_p)$$ (13)

Assuming the difference by a small parameter, $R_n^2/R_p^2 = 1 + \epsilon$, we have

$$\Delta Q_W^{n-p} \simeq N(Z\alpha)^2(0.221\,\epsilon)/q_p$$ (14)

Our RMF calculation gives $\Delta Q_W^{n\ p} = 0.294$ in TM1, $\Delta Q_W^{n\ p} = 0.306$ in NL3, $\Delta Q_W^{n-p} = 0\ 285$ in NL-SH parameters for ^{137}Ba and $\Delta Q_W^{n-p} = 1.301$ inTM1, $\Delta Q_W^{n-p} = 1.354$ in NL3 and $\Delta Q_W^{n-p} = 1\ 274$ in NL-SH parameters for ^{226}Ra.

We next study the parity violations by the 'isotopic ratios'. The dependence of the parity violating amplitude on the atomic theory contribution $\mathcal{A}(Z)$ will cancel out in the ratio of two measurements performed in two different isotopes of the same element, provided the $\mathcal{A}(Z)$ does not change appreciably along the isotopic chain. Unfortunately, although the atomic physics cancels in the ratios but the nuclear structure does not. We consider the following two ratios [31] :

$$\mathcal{R}_1 = \frac{Q_W(N', Z) - Q_W(N, Z)}{Q_W(N', Z) + Q_W(N, Z)}$$

$$\approx \frac{Q_W^{St\ Mod}(N', Z) + Q_W^{nuc}(N', Z) - Q_W^{St\ Mod}(N, Z) - Q_W^{nuc}(N, Z)}{Q_W^{St\ Mod}(N', Z) + Q_W^{nuc}(N', Z) + Q_W^{St\ Mod}(N, Z) + Q_W^{nuc}(N, Z)} \tag{15}$$

and

$$\mathcal{R}_2 = \frac{Q_W(N', Z)}{Q_W(N, Z)} \approx \frac{Q_W^{St\ Mod}(N', Z) + Q_W^{nuc}(N', Z)}{Q_W^{St\ Mod}(N, Z) + Q_W^{nuc}(N, Z)} \tag{16}$$

where $N'(N)$ is the largest (smallest) neutron number. In the above the $\approx$ sign follows from that the q_p remains constant along the whole isotopic chain (see in the Tables). It has been argued in Ref [31] that corrections to Standard Model predictions or uncertainties in the nuclear structure are essentially same whether one uses the $\mathcal{R}_1$ or $\mathcal{R}_2$. We can write the $\mathcal{R}_1$ approximately as

$$\mathcal{R}_1 \approx \frac{Q_W^{St\ Mod}(N', Z) - Q_W^{St\ Mod}(N, Z)}{Q_W^{St\ Mod}(N', Z) + Q_W^{St\ Mod}(N, Z)} \left[1 + \frac{N'}{\Delta N} \Delta q_n \right] \tag{17}$$

where $\Delta N = N' - N$ represents the difference in neutron number and $\Delta q_n = q_n(N', Z) - q_n(N, Z)$ is the difference in q_n's between two extreme isotopic chains. Since the atomic uncertainties have been eliminated from the (17), the remaining uncertainties in $\mathcal{R}_1$ is the known accuracy in the neutron and proton rms radii. While the proton densities have been determined with remarkable accuracy, the precise experimental information on the neutron distributions is lacking. Thus the main nuclear structure uncertainty in the isotopic ratio comes from our limited knowledge of the neutron radii of heavy nuclei. The relative uncertainty in $\mathcal{R}_1$ may be approximated as

$$\frac{\delta \mathcal{R}_1}{\mathcal{R}_1} \approx -\frac{232}{525} (Z\alpha)^2 \frac{N'}{\Delta N} \delta \left[\frac{t(N'Z) - t(N, Z)}{\langle r_p \rangle} \right]. \tag{18}$$

We shall do the following to determine the relative error in $\mathcal{R}_1$ i.e. $\delta \mathcal{R}_1 / \mathcal{R}_1$. We calculate the quantity $\Delta(t) = (t(N'Z) - t(N, Z))/\langle r_p \rangle$ where $(N'Z)$ refers the heaviest member and (N, Z) to the lightest member of the isotope chains and $\langle r_p \rangle$ is the average proton rms radius of the nuclei in the chain. Finally the model spread, $\delta(\Delta(t))$ is calculated in the different parameter sets We found that the relative uncertainty in

the ratio $\mathcal{R}_1$, $\delta\mathcal{R}_1/\mathcal{R}_1$ = 0.00293 for barium isotopes and $\delta\mathcal{R}_1/\mathcal{R}_1$ = 0.00119 for radium isotopes

In conclusion, we have analyzed the Ba and Ra isotopes using a relativistic theory with different interactions and calculated the self-consistent ground state binding energies, the proton and neutron radii. Results have been compared with the available experimental data. We have also studied the nuclear weak charges for Ba and Ra isotopes. Singly charged ions of these atoms have been suggested for possible measurements of PNC Our calculation yields $\Delta Q_W^{n-p}/Q_W$ of 0 38% for ^{137}Ba and 1% for ^{226}Ra It is also seen that the estimated relative uncertainty of the PNC ratios, $\mathcal{R}_1$, in the isotopic chains considered here is around 0.11% – 0.29%. These results will have an important bearing on high precision studies of PNC in a single isotope or a chain of isotopes of Ba$^+$ and Ra$^+$.

References

[1] M A Bouchiat and C Bouchiat *Phys Lett.* **B48** 111 (1974), I B Khriplovich *Pis'ma Zh Eksp Teor Fiz* **20** 686 (1974) [*JETP Lett* **20** 315 (1974)], P G H Sandars *Atomic Physics* (eds) G Zu Pulitz (New York · Plenum) Vol. 4 p71 (1975), D S Sorede and E N Fortson *Bull. Am Phys Soc* **20** 491 (1975)

[2] N H Edwards, S J Phipp, P E G Baird and S Nakayama *Phys Rev Lett* **74** 2654 (1995), D M Meekhof, P K Majumder, S K Lamoreaux and E N Forston *Phys. Rev* **A52** 1895 (1995), M J D Macpherson, K P Zetie, R B Warrington, D N Stacey and J P Hoare *Phys Rev Lett* **67** 2784 (1991)

[3] C S Wood, S C Bennett, D Cho, B P Masterson, J L Roberts, C E Tanner and C E Wieman *Science* **275** 1759 (1997)

[4] V A Dzuba, V V Flambaum and O P Sushkov *Phys Lett.* **A141** 147 (1989)

[5] S A Blundell, W R Johnson and J Sapirstein *Phys Rev Lett* **65** 1411 (1990)

[6] S C Bennett and C E Wieman *Phys Rev Lett* **82** 2484 (1999)

[7] W J Marciano, and J L Rosner *Phys Rev Lett* **65** 2963 (1990), P Langacker, M -X Luo and A K Mann *Rev Mod Phys* **64** 87 (1992); J Erler and P Langacker *Euro J Phys* **1** 90 (1998)

[8] V A Dzuba, V V Flambaum and J S M Ginges *Phys Rev.* **D46** 076013 (2002), and references therein

[9] E N Fortson *Phys. Rev Lett* **70** 2383 (1993)

[10] T W Koerber, M H Schacht, W Nagourney and E N Fortson *J. Phys.* **B36** 637 (2003)

[11] K P Geetha *PhD Thesis* (Bangalore University, India) (2002); B K Sahoo, R Chaudhuri, B P Das and D Mukherjee *Phys Rev Lett* **96** 163003 (2006)

[12] L W Wansbeek, B K Sahoo, R G E Timmermans, K Jungmann, B P Das and D Mukherjee *Phys. Rev* **A78** 050501 (2008)

[13] V A Dzuba, V V Flambaum and J S M Ginges *Phys Rev* **A63** 062101 (2001)

[14] C E Wieman, C Monroe and E A Cornel in *Laser Spectroscopy X* (eds) H Henrikson and P Vogel (World Scientific) (1990)

[15] E N Fortson, Y Pang and L Wilets *Phys. Rev. Lett.* **65** 2857 (1990)

[16] S J Pollock, E N Fortson and L Wilets *Phys Rev* **C46** 2587 (1992)

[17] B Q Chen and P Vogel *Phys Rev* **C48** 1392 (1993)

[18] P K Panda and B P Das *Phys Rev* **C62** 065501 (2000), D Vretenar, G A Lalazissis and P Ring *Phys. Rev.* **C62** 045502 (2000)

[19] J S M Ginges and V V Flambaum *Phys Rep* **637** 63 (2004)

[20] H P Dürr and E Teller *Phys Rev* **101** 494 (1956)

[21] M H Johnson and E Teller *Phys Rev* **98** 783 (1955)

[22] H P Dürr *Phys Rev* **103** 469 (1956)

[23] J D Walecka *Ann Phys* (New York) **83** 491 (1974)

[24] B D Serot and J D Walecka *Adv Nucl Phys.* **16** 1 (1986), *Ibid, Int J Mod Phys* **E6** 515 (1997)

[25] Y K Gambhir, P Ring and A Thimet *Ann Phys* (New York) **198** 132 (1990)

[26] Y Sugahara and H Toki *Nucl. Phys* **A579** 557 (1994)

[27] P Moller *et al, At Data Nucl. Data Tables* **39** 225 (1988)

[28] G Audi and A H Wapstra *Nucl Phys* **A595** 409 (1995)

[29] I Angeli *At data Nucl Data Tables* **87** 185 (2004)

[30] S J Pollock and M C Welliver *Phys Lett* **B464** 177 (1999)

[31] M J Ramsey-Musolf *Phys Rev.* **C60** 015501 (1999); T Sil, M Centelles, X Viñas and J Piekarewicz *Phys. Rev* **C71** 045502 (2005)